PHYSICAL REVIEW E **89**, 013110 (2014)

Head-on collision of dust-acoustic solitons in a strongly coupled dusty plasma

S. K. Sharma, A. Boruah, and H. Bailung

Physical Sciences Division, Institute of Advanced Study in Science & Technology Paschim Boragaon, Guwahati-781035, India

(Received 25 July 2013; published 31 January 2014)

The collision between two counterpropagating dust acoustic solitary waves in a strongly coupled dusty plasma has been observed. The measured velocity and width of the solitary wave agree with the solution of the Korteweg–de Vries equation derived by using the generalized hydrodynamic model. The two counterpropagating solitary waves of equal amplitude merge into a single pulse with twice the individual soliton amplitude and then pass through each other. The solitons suffer a small time delay in propagation after collision. The measured delay time obtained from their trajectories is also presented.

DOI: 10.1103/PhysRevE.89.013110 PACS number(s): 52.27.Lw, 52.27.Gr, 52.35.Sb

I. INTRODUCTION

A dust acoustic wave is the analog of an ion acoustic wave in the very low frequency regime where the dust mass provides the inertia and electrons and ions provide pressure to sustain the wave [1,2]. The nonlinear evolution of the dust acoustic wave into solitons has been well studied theoretically in an unmagnetized weakly coupled dusty plasma [1,3,4]. The effect of strong correlation among the dust particles, which arises when the ratio of intergrain potential energy to the dust thermal energy becomes greater than unity (i.e., the coupling parameter $\Gamma > 1$) [5], on the propagation of the dust acoustic solitary wave (DASW) has also been investigated using various theoretical models (see Ref. [6] and references therein). However, there have been very few experimental investigations of the DASW in laboratories. Bandyopadhyay *et al*. [7] studied the excitation and propagation of the DASW and compared their results with the solution of the Korteweg–de Vries (KdV) equation derived for a weakly coupled dusty plasma [3]. In a monolayer hexagonal dust lattice (for which $\Gamma > \Gamma_c$, where Γ_c is the critical coupling parameter for dust crystallization), solitary waves and their interactions have been studied [8,9].

One important criterion for a solitary wave to be identified as a soliton is that it has to survive a collision (head-on or overtaking) with another solitary wave [10]. In this paper, we report an observation of a head-on collision between two counterpropagating dust acoustic solitons in a strongly coupled dusty plasma in the regime $1 \ll \Gamma < \Gamma_c$.

II. EXPERIMENTAL PROCEDURE

The experiment is performed in a cylindrical glass chamber which is 100 cm in length and 15 cm in diameter. The chamber is first evacuated down to 10^{-4} Pa and then is filled with argon gas to attain a working pressure in the range of 0.1–2 Pa. Discharge is produced by applying rf power (13.56 MHz, 2–10 W) as described in Ref. [11]. A rectangular graphite plate (G) of dimension 30 cm (length) $\times$ 14.5 cm (breadth) $\times$ 0.2 cm (thickness) is kept horizontally inside the chamber with vertical fencing at both ends. Gold coated silica particles of diameter 5 μm and density 2.6 g cm^{-3} are injected into the plasma by using a piezoelectric buzzer fitted below the plate (G). The particles acquire a large amount of negative charge in the plasma and levitate in the plasma sheath boundary region above the plate by balancing gravitational force (downward) and the sheath electrostatic force (upward). The particle cloud is $\sim$2 to 3 mm thick and levitates $\sim$0.8–1 cm above the plate. A horizontal sheet of green laser light (532 nm, 70 mW) is used to illuminate the particles, and their motion is recorded (from top) in a high resolution digital camera with a Nikkor microlens attached to it. The particle cloud undergoes a transition into a highly ordered crystal structure when the chamber pressure is raised above a critical value ($\sim$3 Pa) as observed in Ref. [11]. In this experiment, the working pressure is maintained in the range of 0.5–2.0 Pa so that the particles remain in the fluidlike state, i.e., the coupling parameter Γ lies in the range of $1 \ll \Gamma < \Gamma_c$. Typical values of the plasma parameters are electron and ion densities on the order of 10^8 cm^{-3}, electron temperature $\sim$5 eV, ion temperature $\sim$0.1 eV, dust charge on the order of 10^4 electron charge, and dust density (estimated from the interparticle distance) on the order of 10^3 cm^{-3} [11]. Dust particles are considered to be at room temperature. It is to be noted that the growth of submicron size carbon dust particles due to sputtering of the graphite target has been observed in Ar plasma at 100 W rf power and -300 V dc self bias at the graphite target [12]. However, for the present experimental conditions, i.e., low rf power (6 W) and grounded graphite plate, the possibility of the formation of submicron size particles due to sputtering from the graphite plate is very low.

The dust acoustic wave is excited by applying a continuous small amplitude sinusoidal signal (1–20 Hz) to the exciter E1. The exciter is a 0.6 cm wide graphite section placed on the same horizontal plane of the grounded graphite plate (Fig. 1). A small positive dc offset is also applied to the exciter prior to the application of the excitation signal. This dc offset creates a potential deep filled with particles just above the exciter. The measured wave numbers of the observed waves at different frequencies of the applied signal are found to follow the linear dispersion relation of the dust acoustic wave in the long wavelength limit [1]. The velocity of the observed dust acoustic wave is found to be $\sim$5.0–6.0 cm s^{-1} for the pressure in the range of 0.5–2.0 Pa. Then, instead of a sinusoidal signal, a short negative pulse of amplitude of 5–20 V (100 ms duration) is applied to E1 to excite the DASW. In order to observe collision between two DASWs, the short negative pulse is applied simultaneously to the exciters E1 and E2 which are 5.7 cm apart as shown in Fig. 1. The dimension of E2 is the same as E1.

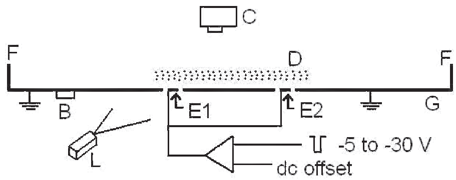

FIG. 1. Schematic of the experimental setup. G: graphite plate; E1 and E2: exciters; D: dust particles; F: fence; B: buzzer; C: camera; and L: laser. To excite the linear dust acoustic wave, a continuous sinusoidal signal is applied to E1. For the excitation of single DASW a negative pulse is applied to E1. E2 and the remaining part of the plate are grounded.

III. THEORY

Considering the generalized hydrodynamic model equation for the strongly coupled dust fluid with Boltzmann distributed electrons and ions [13,14], the KdV equation is derived, which can be expressed in the dimensionless form as

$$\frac{\partial n}{\partial \tau} + Pn\frac{\partial n}{\partial \xi} + Q\frac{\partial^3 n}{\partial \xi^3} = 0, \quad (1)$$

where n is the dust density normalized by its equilibrium value (n_{d0}), the space ξ and time τ coordinates in the wave frame are normalized by the dust Debye length λ_{Dd} [$= (\lambda_{De}^{-2} + \lambda_{Di}^{-2})^{-1/2}$ where $\lambda_{De} = (\varepsilon_0 \kappa T_e / n_{e0} e^2)^{1/2}$ and $\lambda_{Di} = (\varepsilon_0 \kappa T / n_{i0} e^2)^{1/2}$] and the inverse of the dust plasma frequency $\omega_{pd}^{-1} = (\varepsilon_0 m_d / Z_d^2 e^2 n_{d0})^{1/2}$, respectively, n_{e0} (n_{i0}) is the equilibrium electron (ion) density, Z_d and m_d are the charge and mass of the dust particle respectively, and T_e (T_i) is the electron (ion) temperature. The coefficients P and Q in Eq. (1) are given as $P = \frac{2\alpha\lambda + \{\alpha(\mu_e\sigma_i^2 - \mu_i)\lambda/\beta^2\} - \lambda^3\tau_m}{(\alpha - 2\lambda^2\tau_m + \tau_m)}$ and $Q = \frac{\alpha\lambda}{(\alpha - 2\lambda^2\tau_m + \tau_m)}$, where $\alpha = \eta^* - \lambda^2\tau_m$ and $\beta = \mu_e\sigma_i + \mu_i$. Here $\lambda = (1 + \eta^*/\tau_m)^{1/2}$ represents the wave phase velocity normalized by the dust acoustic speed. The parameter η^* is defined as $\eta^* = \eta / m_d n_{d0} \omega_{pd} \lambda_{Dd}^2$, where η is the viscosity coefficient [15]. The viscoelastic relaxation time normalized by ω_{pd}^{-1} is $\tau_m = \eta^*(a/\lambda_{Dd})^2[1 - \gamma_d\mu_d + 4u(\Gamma)/15]^{-1}$, where a is the interparticle distance, γ_d is the adiabatic index, $\mu_d = 1 + u(\Gamma)/3 + (\Gamma/9)\,\partial u(\Gamma)/\partial\Gamma$ is the compressibility, and $u(\Gamma)$ is a measure of the excess internal energy of the system [15]. The parameters μ_e, μ_i, and σ_i are defined as $\mu_e = n_{e0}/Z_d n_{d0}$, $\mu_i = n_{i0}/Z_d n_{d0}$, and $\sigma_i = T_i/T_e$. The value of τ_m, estimated for the present experimental condition, is found to be greater than unity. Therefore, the KdV equation (1) is derived in the limit $\omega_{pd}\tau_m \gg 1$, the so called "kinetic regime." It is to be noted that, in the absence of dust correlation $\eta^* = 0$, Eq. (1) reduces to the KdV equation for a weakly coupled dusty plasma [3].

Equation (1) has a soliton solution of the form $n(\xi,\tau) = n_m \operatorname{sech}^2[(\xi - M\tau)/D]$. The Mach number M (defined as the soliton velocity normalized by the linear dust acoustic velocity) and width D (normalized by the dust Debye length) of the soliton are given by $M = 1 + (P/3)n_m$ and $D = \sqrt{12Q/Pn_m}$ respectively, where n_m represents the amplitude of the soliton.

IV. EXPERIMENTAL RESULTS AND DISCUSSION

A sequence of images showing the propagation of a single compressional pulse is presented in Fig. 2. The two vertical lines appearing to the left of each image are the two edges of the 6 mm exciter E1. The amplitude of the applied pulse in this case is -5 V, and the working pressure is 0.8 Pa. The images are extracted from a video (~2.5 s long) recorded at 30 frames per second (fps). The top image, which is recorded 0.53 s after the video recording starts, shows the two-dimensional view of the undisturbed particles above the plate (and the exciter) just before the excitation. The applied pulse gives an upward push to the particles floating in the potential deep above the exciter. As the vertical motion of the particle is limited within the equilibrium dust levitation height, a density compression is created in the adjacent region in the horizontal plane. The compression is then found to propagate horizontally away from the exciter (when viewed from the top side) as shown in the images recorded at later times (0.80–1.33 s). The compression is identified as a dense and bright region of particles in the respective images.

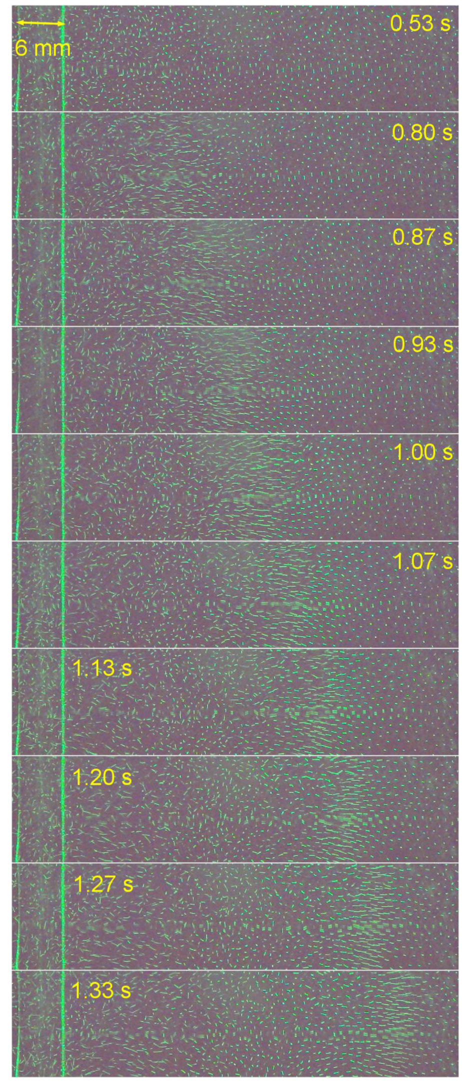

FIG. 2. (Color online) Examples of images recorded at different times (after the video recording starts) showing the propagation of a compressional wave excited by a -5 V pulse. Top image shows the undisturbed particles just before excitation. The compression is identified as a dense and bright region of particles. Two bright vertical lines appearing to the left of each image are the two edges of exciter E1.

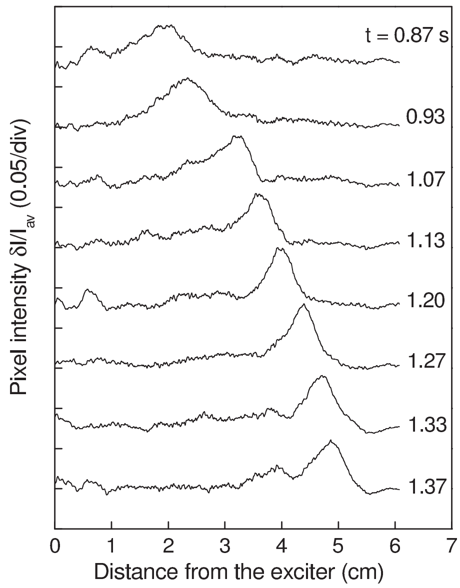

FIG. 3. Spatial evolution of the DASW. Normalized pixel intensity (0.05 per division) versus distance plot of the images recorded at different times. The amplitude of the excitation pulse is −5 V.

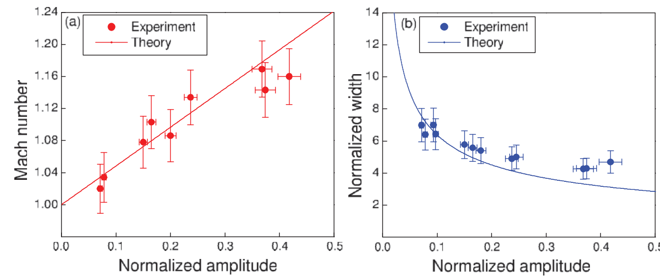

FIG. 4. (Color online) Plot of (a) Mach number and (b) width of the DASW versus wave amplitude. Theoretical values are represented by solid curves.

In order to study the evolution of the observed compressional pulse, we obtain the pixel intensity profile $\delta I/I_{av}$ (which is proportional to dust density perturbation $\delta n_d/n_d$), where $\delta I = I - I_{av}$, of the images (shown in Fig. 2) using IMAGEJ software. Here I_{av} is obtained by averaging intensities (I) of a large number of images [16]. An example of the intensity profiles of images recorded at different times for the −5 V excitation pulse is shown in Fig. 3. The zero of the distance axis corresponds to the right edge of the exciter (Fig. 2). Close to the exciter, the perturbation is wide with the spatial width comparable to the exciter width. As it propagates, the leading part of the pulse steepens (1.07 s), which is balanced by the dispersion effect at a later stage (1.13 s). A fully grown solitary wave is observed at 1.20 s, which travels a further distance maintaining its shape and velocity. The measured amplitude of the DASW is $\delta n_d/n_d$ ($= \delta I/I_{av}$) ~ 0.08, and its velocity is $\sim$6.0 cm s^{-1}. Moving further away from the exciter, the amplitude of the wave decreases with the increase in its width (1.33–1.37 s). The reduction in the wave amplitude is due to the viscous damping. The dust neutral collision frequency (ν/ω_{pd}) for the present working pressure of 0.8 Pa is very small ($\sim$0.07) compared to the viscosity coefficient η^*. It is important to mention here that higher amplitude DASWs (excited by applying higher excitation voltages) take less time to grow, and hence, they are formed at relatively shorter distances. Moreover, for much higher excitation voltages, the perturbation transforms into a shocklike structure at relatively higher pressure.

The Mach number M and the normalized width D (full width at half maxima) of the observed DASW of different amplitudes are measured and are shown in Fig. 4. With the increase in wave amplitude, the Mach number increases linearly [Fig. 4(a)], and its width (D) decreases [Fig. 4(b)] satisfying two distinctive properties of a solitary wave. The measured values show good agreement with the theoretical values (solid curves). The coefficients P and Q are estimated by using the parameters $\mu_e = 10$, $\mu_i = 11$, and $\sigma_i = 0.02$. For the present experimental condition, i.e., Γ just below the critical value Γ_c, the viscosity coefficient η^* is considered to be in the range of 0.3–0.5 [17] and $\tau_m \sim 10$–20. However, the present variation in η^* and τ_m has little effect on coefficients P and Q. The effect of strong dust correlation, taken into account through viscoelastic terms (η^* and τ_m), slightly reduces the absolute values of the coefficients (P and Q) in the KdV equation compared to the case when no correlation is considered.

In order to observe a collision between two DASWs, a negative pulse of amplitude −5 to −15 V is applied simultaneously to both the exciters E1 and E2 (Fig. 1). The applied pulse excites two DASWs of equal amplitude propagating toward each other. Figure 5 shows an example of the observed collision between two such counterpropagating solitary waves excited by a 10 V negative pulse at a pressure

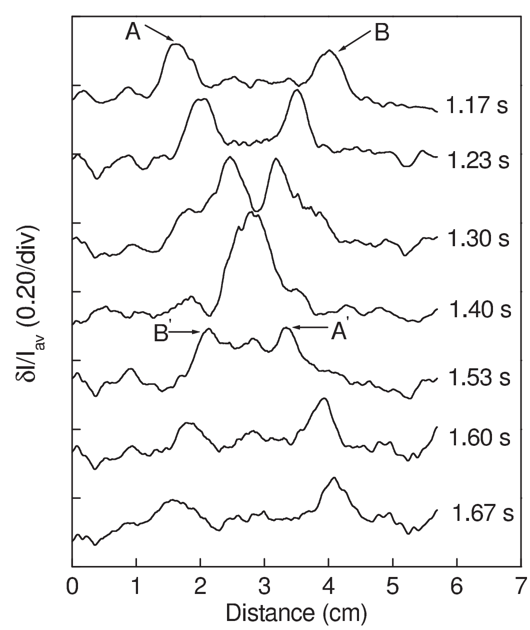

FIG. 5. An example of a pixel intensity profile at different times showing a collision between two counterpropagating DASWs marked as A and B excited by a −10 V pulse. The peaks of the outgoing solitary waves are identified as A′ and B′. Positions $x = 0$ and 5.7 cm correspond to the inner edges of E1 and E2, respectively.

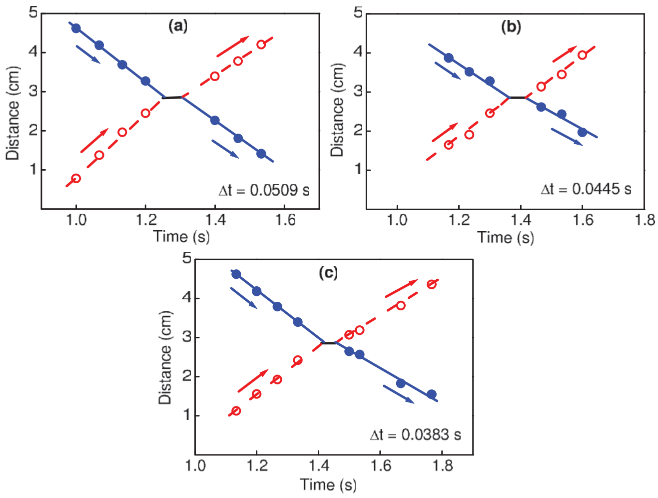

FIG. 6. (Color online) Trajectories of incoming and outgoing DASWs corresponding to excitation voltage (a) −15 V, (b) −10 V, and (c) −8 V. Observed trajectories represented by open circles for soliton A and filled circles for soliton B are fitted to straight lines. The time difference between the intersecting points of incoming and outgoing trajectories is the delay time Δt (indicated by the horizontal solid line).

of ∼1 Pa. The positions $x = 0$ and $x = 5.7$ cm on the distance axis represent the inner edges of E1 and E2, respectively. The incoming DASWs (marked as A and B) interact with each other at a position nearly equidistant from the exciters. The amplitude and Mach number of the incoming DASWs just before the interaction are 0.15 and 1.08, respectively. During the interaction, the two solitary waves merge into a single pulse for a very short time, and then they pass through each other. The maximum amplitude (∼0.31) of the resultant pulse observed (1.40 s) in this case is nearly two times the amplitude of the incoming solitary wave. The outgoing solitary waves (marked as A′ and B′) propagate with a slightly smaller velocity compared to the incoming ones because of the reduction in wave amplitude with time due to the viscous damping. Although asymmetry appears in the shapes of the two outgoing solitary waves, their measured velocities are nearly the same. The asymmetry in the shapes of the two waves (A′ and B′) is thought to be due to the fact that they are now propagating in a medium slightly disturbed by the incoming waves (A and B).

An example of the recorded video at 30 fps showing the head-on collision between two DASWs can be found in the Supplemental Material [18]. The video clearly shows that the counterpropagating DASWs pass through each other after the collision.

The trajectories of incoming and outgoing DASWs are shown in Fig. 6 for three different amplitudes of the applied negative pulse (15, 10, and 8 V). The waves suffer a time delay Δt after collision, which is obtained from the temporal difference between two intersecting points of incoming and outgoing trajectories as shown in Fig. 6. The measured delay time (shown in each plot) is found to decrease with the decrease in the excitation amplitude.

V. CONCLUSION

To summarize, the propagation and collision of the DASW have been observed in a strongly coupled dusty plasma in the regime $1 \ll \Gamma < \Gamma_c$. The dependence of velocity and width of the observed solitary wave with its amplitude follows the relation predicted by the KdV equation derived by using the generalized hydrodynamic model. The major effect of strong dust correlation observed on the propagation of the DASW is the viscous damping as $\nu/\omega_{pd} \ll 1$ in this case. The two counterpropagating DASWs of equal amplitude are found to survive a head-on collision between them, which confirms that the observed solitary waves are solitons. During collision, the two counterpropagating solitons merge into a single pulse momentarily and then pass through each other. The maximum amplitude of the resultant pulse is nearly twice that of the individual soliton amplitude, indicating an apparent linear interaction between them. The present observation is similar to the results reported earlier for the head-on collision of ion-acoustic solitons [10]. The measured delay time during the collisions observed in this experiment depends on the excitation pulse amplitude. Using the simple experimental setup and excitation technique presented here, it is possible to observe linear as well as nonlinear dust acoustic waves and their interaction in a single experimental run. The wave excitation mechanism presented in this experiment is very efficient and has a similarity with the excitation mechanism of an ion-acoustic wave or soliton in a double plasma device [19].

ACKNOWLEDGMENTS

One of the authors, S.K.S., thanks DST, Government of India for supporting the work under the INSPIRE Faculty award. The authors thank Dr. Y. Nakamura for suggestions and support.

[1] N. N. Rao, P. K. Shukla, and M. Y. Yu, Planet. Space Sci. **38**, 543 (1990).
[2] A. Barkan, R. L. Merlino, and N. D'Angelo, Phys. Plasmas **2**, 3563 (1995).
[3] N. N. Rao, Phys. Scr., **T75**, 179 (1998).
[4] P. K. Shukla and A. A. Mamun, New J. Phys. **5**, 17 (2003).
[5] H. Ikezi, Phys. Fluids **29**, 1764 (1986).
[6] P. K. Shukla and B. Eliasson, Phys. Rev. E **86**, 046402 (2012).
[7] P. Bandyopadhyay, G. Prasad, A. Sen, and P. K. Kaw, Phys. Rev. Lett. **101**, 065006 (2008).
[8] D. Samsonov, A. V. Ivlev, R. A. Quinn, G. Morfill, and S. Zhdanov, Phys. Rev. Lett. **88**, 095004 (2002).
[9] P. Harvey, C. Durniak, D. Samsonov, and G. Morfill, Phys. Rev. E **81**, 057401 (2010).
[10] H. Ikezi, R. J. Taylor, and D. R. Baker, Phys. Rev. Lett. **25**, 11 (1970).
[11] S. K. Sharma, R. Kalita, Y. Nakamura, and H. Bailung, Plasma Sources Sci. Technol. **21**, 045002 (2012).
[12] D. Samsonov and J. Goree, J. Vac. Sci. Technol. A **17**, 2835 (1999).

[13] B. M. Veeresha, S. K. Tiwari, A. Sen, P. K. Kaw, and A. Das, Phys. Rev. E **81**, 036407 (2010).

[14] S. Ghosh, M. R. Gupta, N. Chakrabarti, and M. Chaudhuri, Phys. Rev. E **83**, 066406 (2011).

[15] P. K. Kaw and A. Sen, Phys. Plasmas **5**, 3552 (1998).

[16] J. Heinrich, S.-H. Kim, and R. L. Merlino, Phys. Rev. Lett. **103**, 115002 (2009).

[17] S. Ichimaru and S. Tanaka, Phys. Rev. Lett. **56**, 2815 (1986).

[18] See Supplemental Material at http://link.aps.org/supplemental/10.1103/PhysRevE.89.013110 for a visual demonstration of a head-on collision of two counterpropagating DASWs. The video clearly shows the survival of the DASWs after the collision.

[19] K. E. Lonngren, Plasma Phys. **25**, 943 (1983).